Interplay between ER Exit Code and Domain Conformation in CFTR Misprocessing and Rescue

Gargi Roy, Elaine M. Chalfin, Anita Saxena, and Xiaodong Wang

Department of Physiology and Pharmacology, University of Toledo College of Medicine, Toledo, OH 43614

Multiple mutations in cystic fibrosis transmembrane conductance regulator (CFTR) impair its exit from the endoplasmic reticulum (ER). We compared two processing mutants: ΔF508 and the ER exit code mutant DAA. Although both have severe kinetic processing defect, DAA but not ΔF508 has substantial accumulation in its mature form, leading to higher level of processing at the steady state. DAA has much less profound conformational abnormalities. It has lower Hsp70 association and higher post-ER stability than ΔF508. The ER exit code is necessary for ΔF508 residual export and rescue. R555K, a mutation that rescues ΔF508 misprocessing, improves Sec24 association and enhances its post-ER stability. Using in situ limited proteolysis, we demonstrated a clear change in trypsin sensitivity in ΔF508 NBD1, which is reversed, together with that of other domains, by low temperature, R555K or both. We observed a conversion of the proteolytic pattern of DAA from the one resembling ΔF508 to the one similar to wild-type CFTR during its maturation. Low temperature and R555K are additive in improving ΔF508 conformational maturation and processing. Our data reveal a dual contribution of ER exit code and domain conformation to CFTR misprocessing and underscore the importance of conformational repair in effective rescue of ΔF508.

INTRODUCTION

Cystic fibrosis (CF) is an inherited disease caused by impaired plasma membrane chloride conductance mediated through the cystic fibrosis transmembrane conductance regulator (CFTR; Riordan et al., 1989). CFTR is a member of the ATP-binding cassette (ABC) family of transporters, and is composed of two homologous modules linked by a regulatory (R) domain (Riordan et al., 1989). Each module consists of a membrane-spanning domain (MSD) and a nucleotide-binding domain (NBD). Deletion of the phenylalanine at residue 508 (ΔF508) within NBD1 is present in over 90% of CF patients. ΔF508 CFTR fails to be efficiently transported from the endoplasmic reticulum (ER) to the Golgi and thus is not processed to the mature glycoforms (Cheng et al., 1990). Instead, it is degraded through the ubiquitin proteasome pathway (Jensen et al., 1995; Ward et al., 1995). The ΔF508 transport defect is temperature sensitive as the mutant CFTR is exported to the cell surface more efficiently at reduced temperature (Denning et al., 1992). The temperature-rescued ΔF508 CFTR has reduced stability at the cell surface when shifted back to physiological temperature (Lukacs et al., 1993).

The vesicle-mediated export of cargo proteins from the ER depends on the coatomer complex II (COPII; Barlowe et al., 1994). The di-acidic motif in the cytoplasmic domain is a widely used cargo concentration signal for COPII-mediated ER export (Nishimura and Balch, 1997). Sec24 subunit of COPII specifically recognizes the di-acidic code (Miller et al., 2002; Mossessova et al., 2003). A "DAD" ER exit motif was identified within CFTR NBD1, and substitution of the second aspartic acid with an alanine (resulting in DAA) abolishes the association of CFTR with Sec24 and dramatically reduces the kinetic processing of CFTR from the ER (Wang et al., 2004).

The mechanism of ΔF508 misprocessing remains unclear. Both dominant retention (Chang et al., 1999) and defective export (Wang et al., 2004) have been proposed. In support of the former, multiple arginine-framed (RXR) ER retention motifs widely used among the oligomeric potassium channels (Zerangue et al., 1999) were identified in CFTR, whose substitution leads to ΔF508 rescue (Chang et al., 1999; Hegedus et al., 2006). In a screen for ΔF508 revertants, substitution of either arginine in the RXR motif at residue 553–555 in NBD1 rescues ΔF508 (Teem et al., 1993, 1996). In support of defective export, ΔF508 CFTR has reduced association with Sec24, which is reversed upon reducing the temperature (Wang et al., 2004). Although the folding of the multiple domains of CFTR occurs largely cotranslationally (Kleizen et al., 2005), ΔF508 CFTR has a specific defect in conformational maturation within the ER (Lukacs et al., 1994). Given its defective conformation, the usage of sorting signals in the context of ΔF508 CFTR is unknown, neither is the impact of the disruption of sorting motifs on CFTR conformation.

A significant amount of work has been conducted to address the conformational defect of ΔF508 CFTR. The deletion of F508 impacts the folding kinetics of isolated NBD1 (Qu et al., 1997; Serohijos et al., 2008b), but no major structural change has been observed in ΔF508 NBD1 based on structural analysis (Lewis et al., 2005; Thibodeau et al., 2005). Compared with the isolated NBD1, the processing of full-length CFTR appears to be more susceptible to F508 substitution mutations (Du et al., 2005; Thibodeau et al., 2005). In fact, the deletion of F508 has a global impact on the conformation of multiple domains including the MSDs and NBD2 (Zhang et al., 1998; Chen et al., 2004; Du et al., 2005; Cui et al., 2007; Du and Lukacs, 2009). Furthermore, F508 was recently

predicted to reside at the interface between NBD1 and the cytoplasmic loop 4 within MSD2 (Serohijos *et al.*, 2008a). How F508 deletion leads to the global conformational change through the NBD1-MSD2 contact remains to be determined.

To understand the relationship between sorting signals and domain conformation in ΔF508 misprocessing and rescue, we systematically compared the biochemical properties of two different CFTR-processing mutants: ΔF508 and DAA, and tested the effects of different ΔF508 rescue maneuvers. We provide evidence supporting DAA as a sorting mutant with no major conformational defect and ΔF508 as a conformational mutant with a partially functional ER exit code. We found that disruption of the ER exit code alone produces only a mild misprocessing phenotype at the steady state, whereas the conformational mutant impairs both export and post-ER stability, leading to severe misprocessing. In the context of ΔF508 CFTR, where export is compromised to start with, the exit code is absolutely essential for ΔF508 CFTR rescue. Rescue of ΔF508 CFTR is associated with increased coupling to COPII and enhanced post-ER stability. We identified a clear change in trypsin sensitivity in ΔF508 NBD1. Strikingly, this and the trypsin sensitivity of other domains are cooperatively reversed during ΔF508 rescue. Our data are consistent with interplay between ER exit code and domain conformation in CFTR misprocessing and rescue, and emphasizing the importance of domain conformation in not only ER export but also post-ER stability, both of which dictate the steady-state accumulation of mature CFTR, a factor that determines the degree of functional defect in CF.

MATERIALS AND METHODS

CFTR Expression Plasmids

CFTR expression plasmids pcDNA3.1(+)-CFTR-WT and pcDNA3.1(+)-CFTR-ΔF508 harboring human full-length wild-type (WT) and ΔF508 CFTR coding sequences, respectively, were the bases for constructing other CFTR mutants. We used a BspeI-HpaI fragment encompassing NBD1 and R domain of CFTR as a cassette to construct the NBD1 substitution mutants used in this study. Plasmid pcDNA3.1(+)-CFTR-DAA was constructed by replacing the BspeI-HpaI fragment in pcDNA3.1(+)-CFTR-WT with the corresponding fragment from plasmid pTM-1-CFTR-DAA. Other substitution mutants were introduced into NBD1 by overlapping PCRs. The pcDNA3.1(+)-CFTR-ΔF508/R555K and pcDNA3.1(+)-CFTR-ΔF508/DAA were constructed by introducing R555K and DAA, respectively, into pcDNA3.1(+)-CFTR-ΔF508. The pcDNA3.1(+)-CFTR-ΔF508/R555K/DAA was constructed by introducing DAA into pcDNA3.1(+)-CFTR-ΔF508/R555K. To construct pcDNA3.1(+)-CFTR-ΔF508/R29K, an NdeI-BspeI fragment including the 5′ untranslated region, the amino terminal tail (NT) and MSD1 of CFTR was used as a cassette, and R29K substitution was introduced into pcDNA3.1(+)-CFTR-ΔF508 using this cassette. Finally, the pcDNA3.1(+)-CFTR-ΔF508/R29K/R555K was constructed by replacing the BspeI-HpaI fragment of pcDNA3.1(+)-CFTR-ΔF508/R29K with the corresponding fragment from pcDNA3.1(+)-CFTR-ΔF508/R555K. All of the CFTR expression plasmids constructed were verified by sequencing analysis.

Anibodies and Chemicals

CFTR mAbs MM13-4 (recognizing an epitope within residues 25–36 in NT) and M3A7 (recognizing NBD2 and part of the carboxy terminus) were purchased from Millipore (Billerica, MA). CFTR mAbs 13-1 (recognizing the R domain) and 24-1 (recognizing the carboxy terminus) were prepared from the culture supernatants of specific hybridoma cell lines from ATCC (Manassas, VA). Anti-Sec24 polyclonal antibodies were kindly provided by Dr. William Balch (Wang *et al.*, 2004). Anti-Hsp70 polyclonal antibodies and the anti-Hsc70 mAb 1B5 were purchased from Stressgen (Victoria, BC, Canada). Anti-actin mAb C4 was purchased from Millipore (Temecula, CA). Protein G Sepharose 4 Fast Flow was purchased from GE Healthcare (Piscataway, NJ). Cycloheximide (CHX) and brefeldin A (BFA) were purchased from Sigma (St. Louis, MO).

Cell Culture and Transfection

Human embryonic kidney 293 (HEK293) cells stably expressing wild-type or ΔF508 CFTR (Silvis *et al.*, 2003) were maintained in DMEM supplemented

with 10% fetal bovine serum (FBS), 100 U/ml each of penicillin and streptomycin, and 150 μg/ml hygromycin B (EMD Chemicals, Gibbstown, NJ). Baby hamster kidney (BHK) cells stably expressing wild-type (BHK-WT) or ΔF508 CFTR (BHK-ΔF; Seibert *et al.*, 1995) were cultured in DMEM supplemented with F12, 5% FBS, 100 U/ml each of penicillin and streptomycin, and 500 μM methotrexate (Ben Venue Laboratories, Bedford, OH). Cell transfection was performed using Lipofectamine 2000 (Invitrogen, Carlsbad, CA). HEK293 cells stably expressing DAA, ΔF508/DAA and ΔF508/R555K CFTR were generated by transfecting HEK293 cells with specific CFTR expression plasmids and selecting in the presence of 400 μg/ml G418 (A. G. Scientific, San Diego, CA). The generated HEK293 stable cell lines were maintained in DMEM supplemented with 10% FBS, 100 U/ml each of penicillin and streptomycin, and 200 μg/ml G418. BHK cells stably expressing ΔF508/R555K CFTR (BHK-ΔF/R555K) were generated by transfecting BHK cells with the CFTR expression plasmid and selecting with 400 μg/ml G418. The generated BHK stable cell line was maintained in DMEM supplemented with F12, 5% FBS, 100 U/ml each of penicillin and streptomycin, and 200 μg/ml G418.

Assessing CFTR Post-ER Stability

The relative post-ER stability of wild-type and mutant CFTR was assessed by determining the relative turnover rate of CFTR band C in the presence of CHX. HEK293 cells stably expressing various forms of CFTR were incubated in media containing 100 μg/ml CHX at 37°C. At different time points, cells were removed from incubation and lysed. Equal amounts of cell lysates were immunoblotted for CFTR and actin. Cell lysis, protein assay, and immunoblotting were performed as described previously (Wang *et al.*, 2008). Multiple exposures were taken to ensure that the intensity of bands is within the dynamic range. The level of CFTR in band C was quantified by densitometry using ImageJ software (http://rsb.info.nih.gov/ij/; National Institutes of Health) and normalized to the level of actin at each time point. The obtained values were converted to percentage of the value at 0 time point for each construct. As CHX blocks the synthesis of all cellular proteins including actin, the derived turnover rate for CFTR band C is relative to the turnover rate of actin.

Quantitative CFTR Coimmunoprecipitation

HEK293 cells transiently transfected with expression plasmids of different forms of CFTR were washed with ice-cold phosphate-buffered saline and lysed in 50 mM Tris-HCl (pH 7.4), 150 mM NaCl, and 1% Triton X-100 (vol/vol), supplemented with Complete protease inhibitor cocktail (Roche Diagnostics, Mannheim, Germany). CFTR was immunoprecipitated with protein G Sepharose beads coated with CFTR mAb M3A7 or 13-1 as described previously (Wang *et al.*, 2008). The immunoprecipitated proteins were eluted with 50 mM Tris-HCl (pH 6.8) and 1% SDS. Equal proportions of the eluted materials were loaded on a 7.5% gel and immunoblotted for Sec24, Hsp70s, or CFTR. Mock-transfected HEK293 cells served as negative control for proteins nonspecifically associated with the CFTR-antibody–coated protein G Sepharose beads. CFTR and associated proteins were quantified by densitometry as described above. The levels of the associated proteins were subtracted by that of the negative control and then were normalized to the level of CFTR in band B.

In Situ Limited Proteolysis

Microsomes were prepared from CFTR-expressing cells by homogenization and differential centrifugation (Plutner *et al.*, 2005). When necessary, microsomes were incubated in 2.5 M urea on ice as described (Aridor *et al.*, 1998) to remove peripheral membrane proteins. Limited proteolysis was performed largely as described by Zhang *et al.* (1998). Intact microsomes at a final protein concentration of 6.8 mg/ml or equivalent amount of urea-washed microsomes were digested with increasing concentrations of trypsin (Sigma, St. Louis, MO) for 15 min on ice. Then, 5 mM PMSF was added to terminate the reaction and sample buffer was added to solubilize the proteins. Equal amount solubilized digestion mixtures were analyzed by 12% SDS-PAGE and immunoblotted with CFTR domain-specific mAbs.

RESULTS

DAA Has Substantial Accumulation in Post-ER Compartments

Both ΔF508 and DAA have a severe kinetic processing defect from the ER-localized core glycoform (band B) into the Golgi specific complex glycoform (band C) as assessed by pulse-chase analysis (Wang *et al.*, 2004). At the steady state, however, there is greater accumulation of DAA in band C than ΔF508 (Figure 1A). This difference is apparent 24 h after transfection (top panel) and continues to increase to the steady state (bottom panel). We observed the time-dependent accumulation of CFTR in bands B and C after transient transfection in HEK293 cells. Significant synthesis of CFTR
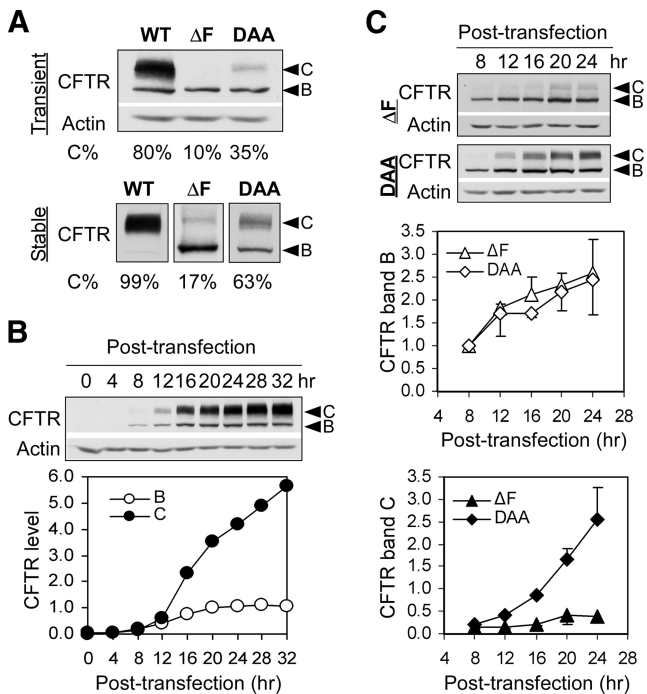
Figure 1. DAA has greater post-ER accumulation than ΔF508. (A) Top, HEK293 cells were transiently transfected with wild-type (WT), ΔF508 (ΔF), and DAA CFTR. After 24 h at 37°C, cells were lysed and equal amounts of lysates were immunoblotted for CFTR. CFTR levels in core glycoform (band B) and complex glycoform (band C) were quantified by densitometry. Percentage of band C of the total was calculated for each CFTR construct. Bottom, HEK293 cells stably expressing the indicated forms of CFTR were lysed. The lysates were immunoblotted for CFTR, and the level of CFTR was quantified as above. (B) HEK293 cells were transiently transfected with WT CFTR. At the indicated time after transfection, cells were lysed, and the lysates were immunoblotted for CFTR. The level of CFTR in bands B and C was quantified by densitometry. (C) The synthesis and maturation of DAA and ΔF CFTR were followed in HEK293 cells between 8 and 24 h after transfection. CFTR levels in bands B and C were quantified by densitometry and normalized to the levels of actin. To facilitate comparison, all values of an individual CFTR construct were further normalized to the value of band B at the first time point. The time courses have been performed twice independently. Representative immunoblotting images are shown on the top, and the means and SEMs are plotted in the charts below.

occurs 8 h after transfection (Figure 1B). Although the level of wild-type band B saturates at 20 h, the level of band C continues to increase beyond 32 h, largely because of the longer half-life for band C (~22 h; Sharma *et al.,* 2001) than band B (<3 h; Wang *et al.,* 2004). ΔF508 and DAA show similar kinetic accumulation in band B but strikingly different rates of accumulation in band C (Figure 1C). ΔF508 band C saturates at 20 h, whereas DAA continues accumulate beyond 24 h. This difference may be attributed to differences in post-ER stability and/or export efficiency between the two processing mutants. As the residual processing of ΔF508 and DAA was hardly detectable using pulse-chase analysis (Wang *et al.,* 2004), we compared the post-ER stability of wild-type, DAA, and ΔF508 CFTR by incubating HEK293 cells stably expressing the corresponding CFTR constructs with CHX and assessing the turnover of their band C. DAA is much more stable than ΔF508 in post-ER compartments (Figure 2), which significantly contributes to its greater accumulation in band C.

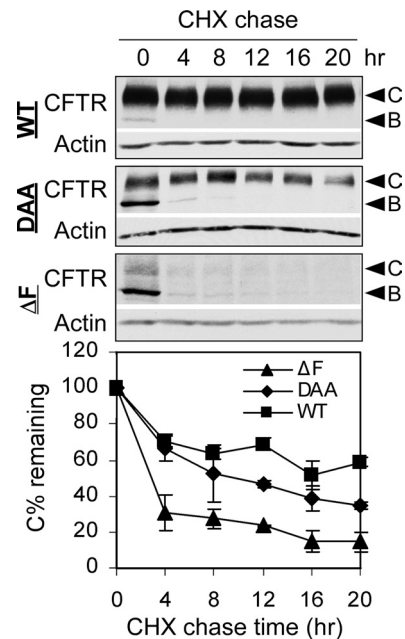**Figure 2.** DAA is much more stable than ΔF508 in post-ER compartments. HEK293 cells stably expressing WT, DAA, or ΔF were incubated with 100 μg/ml CHX for the indicated time periods. Cells were then lysed, and the lysates were immunoblotted for CFTR. CFTR levels in band C were quantified, normalized to actin, and expressed as the percentage of the value at the 0 time point. The experiments were conducted twice. Representative immunoblotting images are shown above, and the means and the SEMs are displayed below.

Compared with ΔF508, DAA Has Far Less Conformational Deviation from Wild-Type CFTR

DAA is defective in ER exit code (Wang *et al.,* 2004). Whether the same amino acid substitution causes significant conformational change in CFTR is not known. We examined the domain conformation of wild-type, ΔF508, and DAA using in situ limited proteolysis. When probed with MM13-4, an mAb recognizing an epitope at the amino terminus of CFTR, DAA displays a pattern that is more close to wild-type than ΔF508 (Figure 3A, a–c). This is evident in the patterns of the 50-kDa (upper rectangles) and 42-kDa (gray arrowhead) fragments and the presence of a 37-kDa fragment (black arrowheads) at high trypsin concentrations (lanes 7 and 8). Of note, a faint 37-kDa band present in ΔF508 even in the absence of trypsin represents an endogenous CFTR degradation product (b, asterisk). This band, whose intensity decreases with increasing trypsin concentration, is distinct from the 37-kDa band that appears and continues its existence at the two highest trypsin concentrations in both wild-type and DAA CFTR (a and c, lanes 7 and 8). Based on the location of MM13-4 epitope, the 37- and 42-kDa fragments contain the amino terminal tail (NT) and MSD1, and the 50-kDa fragment extends into NBD1 (Figure 3B). The observed differences in trypsin sensitivity between wild-type and ΔF508 in the amino-terminal module of CFTR are largely consistent with recent work by Du and coworkers, which demonstrated that multiple CFTR processing mutants including ΔF508 share common conformational defects in NT-MSD1-NBD1 (Du and Lukacs, 2009). As DAA displays a tryptic pattern similar to wild-type CFTR but distinct from all these processing mutants, the impact of DAA mutation on CFTR domain conformation is much minor.
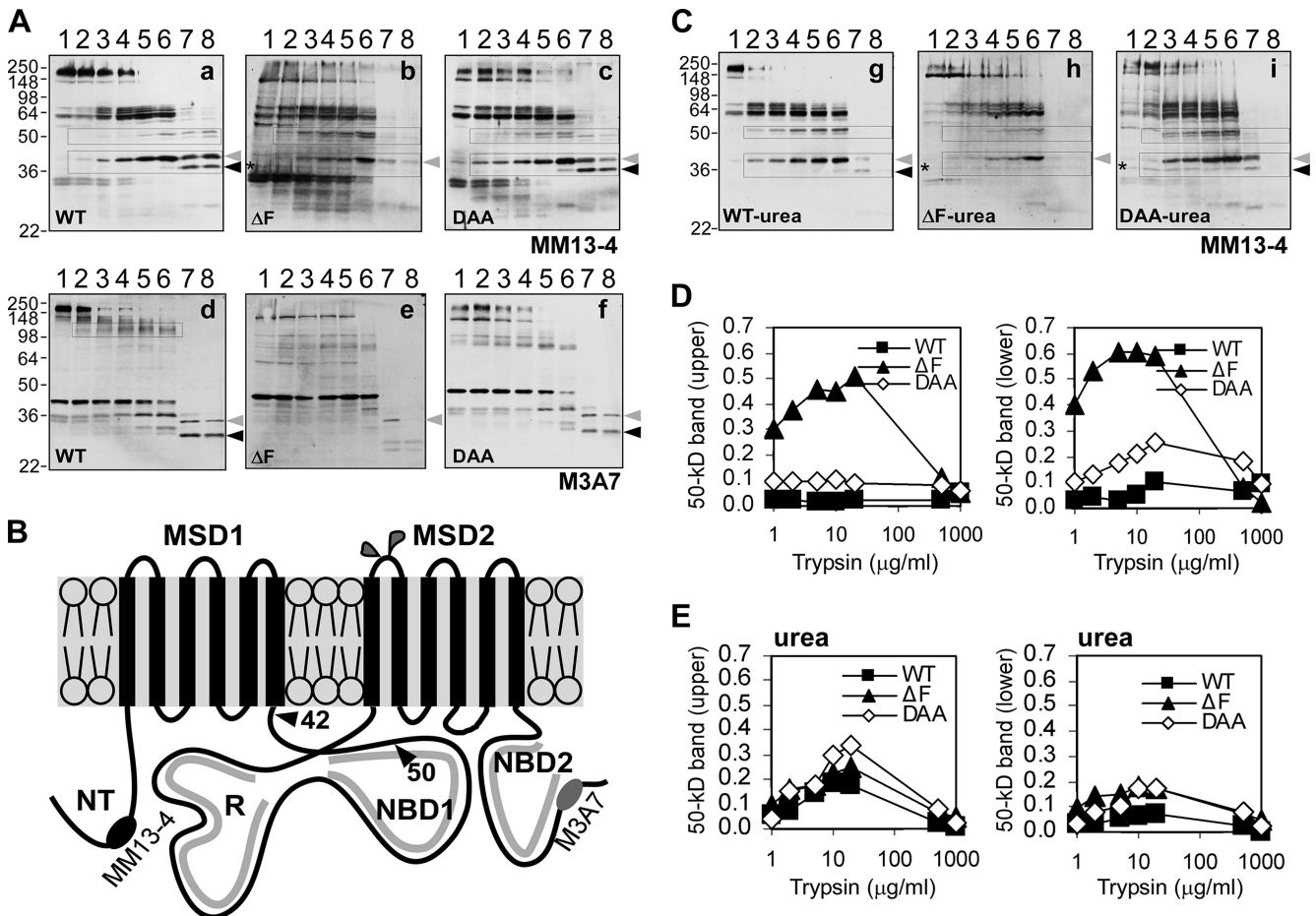
Figure 3. DAA has minimal conformational deviation from wild-type CFTR when compared with ΔF508. (A) Equal amounts of microsomes prepared from HEK293 cells stably expressing the indicated CFTR constructs were subjected to digestion at increasing trypsin concentration. The digestion mixtures were immunoblotted with CFTR mAb MM13-4 (a–c) or M3A7 (d–f). The trypsin concentrations are 0, 0.5, 1, 2.5, 5, 10, 250, and 500 µg/ml. The 42- and 37-kDa fragments in a–c were labeled with gray and black arrowheads, respectively, and the 34- and 30-kDa fragments in d–f were labeled with gray and black arrowheads, respectively. (B) Cartoon of CFTR showing domains, antibody epitopes, glycosylation sites, and the predicted trypsin cleavage sites that generate the 50- and 42-kDa fragments when probed by MM13-4. (C) Microsomes prepared from HEK293 cells stably expressing WT, ΔF, or DAA were subjected to urea wash followed by in situ limited proteolysis and then immunoblotting with MM13-4. (D) The ~50-kDa bands in A, a–c, were quantified by densitometry and normalized to the total level of CFTR in the absence of trypsin (lane 1). (E) The ~50-kDa bands in C were quantified in the same manner.

Because of misprocessing, a greater proportion of ΔF508 or DAA are degraded through the ER-associated degradation (ERAD) than wild-type CFTR. As a result, ΔF508 and, to a lesser extent, DAA have higher levels of endogenous CFTR degradation products at ~33 kDa than wild-type CFTR (Figure 3A, a–c, lane 1). The group of tryptic fragments smaller than 33 kDa, whose intensity corresponds to the that of the 33-kDa endogenous proteolytic fragments, are likely to represent the tryptic degradation products of the 33-kDa band. Moreover, the 33-kDa endogenous proteolytic fragments and their degradation products were almost completely removed by urea wash of the microsomes before trypsin treatment (Figure 3C, g–i), suggesting that the 33-kDa endogenous proteolytic fragments are but peripherally associated with the microsome membrane.

As the 50-kDa fragments extend into NBD1 (Figure 3B), changes in their patterns might reflect changes in NBD1 conformation. We quantified the upper and lower 50-kDa bands by densitometry and normalized them to the total level of CFTR in the absence of trypsin (Figure 3D). The levels of the 50-kDa bands in ΔF508 increase dramatically at

lower trypsin concentrations but decline rapidly at higher trypsin concentrations. In contrast, the changes in the levels of the same bands in wild-type and DAA CFTR are much less. These are consistent with higher trypsin sensitivity for ΔF508 NBD1. DAA NBD1 has slightly increased trypsin sensitivity than wild-type but far less than that of ΔF508 NBD1.

To explore the impact of potential protein–protein interactions on the tryptic sensitivity of CFTR, we washed the CFTR-harboring microsomes with urea to remove associated peripheral proteins before in situ limited proteolysis (Figure 3C). Overall, urea wash increases the trypsin sensitivity for all three forms of CFTR. This is reflected in the reduction of band intensity at higher trypsin concentrations. Despite this, the difference in the presence of the 37-kDa band remains between wild-type and ΔF508 CFTR, suggesting that such difference is definitely independent of CFTR's interactions with other proteins. Interestingly, we have observed a "neutralizing" effect for urea wash on the trypsin sensitivity of NBD1 among different forms of CFTR (Figure 3E).

It has been well established that ΔF508 mutation alters the NBD2 conformation, leading to the disappearance of a ~30-kDa tryptic fragment (Figure 3Ad, black arrowhead) characteristic of wild-type CFTR conformation when probed with M3A7, a mAb recognizing NBD2 and the carboxy terminal tail of CFTR (Zhang *et al.*, 1998; Du *et al.*, 2005; Du and Lukacs, 2009). The same 30-kDa band is present in DAA (Figure 3Af, black arrowhead). Of note, the ~100-kDa bands present in wild-type (Figure 3Ad, rectangle) but not in DAA (Figure 3Af) are derived from the extremely high abundant band C in wild-type CFTR. In DAA, the ~80-kDa bands derived largely from band B are more prominent because of its much lower abundance in band C compared with wild-type CFTR. Consistent with the above prediction, upon treatment with BFA, the 100-kDa fragments from wild-type CFTR are shifted to 80 kDa (Supplemental Figure 1B, c and d).

Taken together, the above results indicate that although ΔF508 causes global conformational alteration in CFTR, the impact of DAA on the domain conformation of CFTR is rather limited.

Maturation of DAA CFTR Is Accompanied by Global Conformational Changes

At the steady state, wild-type CFTR is predominantly present in band C, and ΔF508 largely exists in band B. To test the contribution of state of glycosylation to the different tryptic patterns between wild-type and ΔF508 CFTR, we treated cells expressing wild-type CFTR with BFA before proteolysis. Aside from slightly higher overall trypsin sensitivity after BFA treatment, the key patterns hold when probed with MM13-4 (Supplemental Figure 1A). When probed with M3A7, no major pattern change occurs except for the 100- to 80-kDa shift due to altered state of glycosylation (Supplemental Figure 1B).

Because of the fast maturation kinetics for wild-type CFTR (Figure 1B), it is difficult to capture a time point at which the vast majority of CFTR is in its immature form without significantly compromising the yield of CFTR required for proteolysis. As DAA has minimal conformational deviation from wild-type CFTR but has slower maturation kinetics, we explored the possibility of using DAA as an example to observe the relationship between its maturation and its trypsin sensitivity. We compared the tryptic patterns of DAA at an earlier stage of maturation, the steady-state DAA and the mature form of DAA. To obtain DAA at earlier stage of maturation (DAA-early), we transiently transfected HEK293 cells with DAA CFTR and harvesting cells 12 h after transfection. According to Figure 1C, at this time point, sufficient DAA CFTR has been synthesized but its degree of maturation is much lower than the later time points. To obtain DAA CFTR that is devoid of immature form, we treated HEK293 cells stably expressing DAA CFTR with CHX for 12 h before microsomes were prepared for proteolysis (DAA-CHX). Interestingly, DAA-early displays a tryptic pattern that is more similar to ΔF508 than the steady-state DAA, whereas DAA-CHX is more like wild-type, with the caveat that after CHX treatment, the overall trypsin sensitivity is higher (Figure 4A, a-f). When the 50-kDa fragments were quantified, we found a maturation-dependent pattern change, where the DAA-early resembles ΔF508, the DAA-CHX resembles wild-type, and the steady-state DAA is in between (Figure 4B). This clearly suggests a conformational maturation in NBD1 as well as other domains of DAA CFTR. Thus, although ΔF508 mutation arrests CFTR conformational maturation in an early folding intermediate (Lukacs *et al.*, 1994; Zhang *et al.*, 1998), DAA mutation does not.
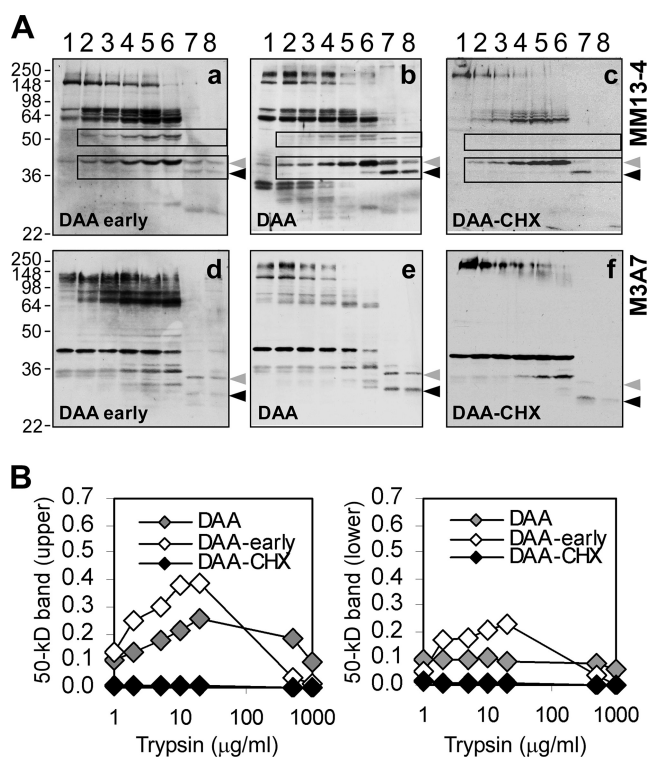

Figure 4. Global conformational changes accompany DAA maturation. (A) Microsomes derived from HEK293 cells harboring DAA CFTR at different stages of maturation were subjected to in situ limited proteolysis. To capture DAA at an earlier stage of maturation, HEK293 cells were transiently transfected with DAA CFTR, and microsomes were prepared 12 h after transfection (DAA early). To remove the immature form (band B) of DAA CFTR, HEK293 cells stably expressing DAA were treated with CHX for 12 h before microsome preparation (DAA-CHX). (B) The ~50-kDa bands in A, a–c, were quantified as described above.

ER-localized DAA Has a Much Lower Association with Hsp70s than ΔF508

ΔF508 is defective in conformational maturation within the ER (Lukacs *et al.*, 1994). Hsp70 associates with the immature form of wild-type CFTR in the ER and dissociates upon transport to the Golgi (Yang *et al.*, 1993). ΔF508 associates with Hsp70 more extensively than wild-type CFTR (Meacham *et al.*, 1999). We conducted quantitative coimmunoprecipitation on HEK293 cells expressing wild-type, DAA or ΔF508 CFTR. To focus on the ER-localized CFTR, all CFTR expressing cells were treated with BFA to block the ER-to-Golgi transport. As shown in Figure 5, DAA has a much lower association with cytoplasmic Hsp70s than ΔF508. The relatively higher levels of Hsp70 and Hsc70 association of DAA than wild-type CFTR might be attributable to its lower accumulation of conformationally mature, but BFA-blocked, CFTR molecules than wild-type CFTR.

The "DAD" Exit Code Remains Functional in the Context of ΔF508 CFTR

Because conformational change can alter the usage of sorting signals, we tested whether the "DAD" motif remains functional as the ER exit signal in the context of ΔF508 CFTR. Introduction of the DAA mutation into ΔF508 CFTR significantly reduced the residual processing of ΔF508 CFTR, as reflected in an unchanged level of band B but a significant reduction in the level of band C (Figure 6A). Because of the
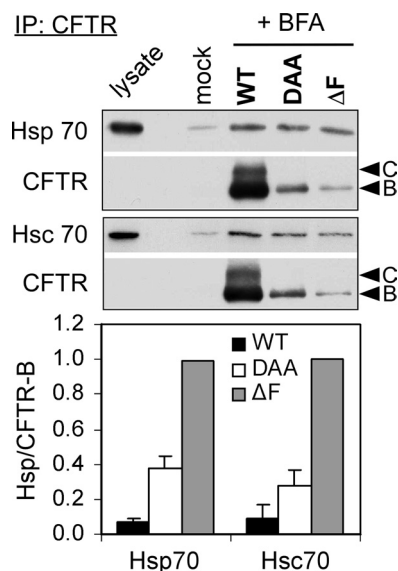
Figure 5. DAA has much lower association with Hsp70s than ΔF508. HEK293 cells were transiently transfected with WT, DAA, or ΔF CFTR. Sixteen hours after transfection, BFA was added at 10 μg/ml, and the cells were incubated at 37°C for an additional 24 h. Mock transfected HEK293 cells served as control (mock). The cells were lysed and coimmunoprecipitation was conducted using protein G beads coated with CFTR mAb 13-1 as described in *Materials and Methods.* A small fraction of mock cell lysate (lysate) and equal proportions of the immunoprecipitated proteins were separated by SDS-PAGE and immunoblotted for the Hsp70s and CFTR. The levels of Hsp70s were subtracted by those of the mock and then normalized to the level of CFTR in band B. Two independent experiments were performed. To facilitate data analysis, the levels of Hsp70-association for WT and DAA were normalized to that of ΔF in each individual experiment, and then the means and SEMs were calculated. Representative immunoblotting images are shown above, and the means and SEMs are plotted below.

wide difference between the intensity of bands B and C, different exposures were used for the quantification of the two bands. At reduced temperature, DAA mutation dramatically reduced the level of band C but only slightly reduced the level of band B, suggesting reduced processing (Figure 6B). The reduction in the level of band C can be caused by reduced export or post-ER stability. We tested the ability of ΔF508/DAA to associate with Sec24 by coimmunoprecipitation and found that it has a significantly lower association with Sec24 than ΔF508 CFTR (Figure 6C). Although the amounts of the Sec24 coimmunoprecipitated from the cell lysates were similar between ΔF508 and ΔF508/DAA, more ΔF508/DAA CFTR was immunoprecipitated than ΔF508 CFTR. Therefore reduction in coupling to COPII contributes to the reduced processing in ΔF508/DAA.

To compare the kinetics of the temperature-dependent processing, we subjected HEK293 cells stably expressing DAA, ΔF508, or ΔF508/DAA to 30°C time course and quantified the levels of bands B and C. To facilitate comparison between different CFTR constructs, we normalized the levels of band B or C at different time points to the level of band B at time 0. We found that DAA itself does not display temperature-dependent export except an initial stabilization of band B, which is followed by a slight "catch-up" in band C (Figure 6D), and introduction of DAA almost completely abolished the temperature-dependent export of ΔF508 CFTR (Figure 6, E and F).

Although DAA has only limited impact on the conformation of wild-type CFTR (Figure 3A), the impact of DAA on ΔF508 CFTR conformation has not been examined. We conducted in situ limited proteolysis on ΔF508 and ΔF508/DAA and found no major conformational change (Figure 6, G and H). Therefore, it is highly unlikely that the introduction of DAA impairs ΔF508 processing at both 37 and 30°C by altering CFTR conformation. Taken together our data support that the "DAD" motif remains functional as the ER exit code in the context of ΔF508 CFTR.

R555K Rescues ΔF508 CFTR by Improving Both Export and Post-ER Stability

R555K, alone (Teem *et al.*, 1996) or in combination with R29K (Hegedus *et al.*, 2006) rescues ΔF508 CFTR. We found that R29K does not improve ΔF508 processing, nor does it contribute to ΔF508 rescue when combined with R555K (2RK) in HEK293 cells and this is true at both 37 and 30°C (Figure 7A). In BHK cells, R29K alone inhibits ΔF508 processing but only slightly enhances ΔF508 processing when combined with R555K at 37°C (Supplemental Figure 2). Of note, in HEK293 cells, the combination of low temperature and R555K additively increases the processing of ΔF508 based on the percent of total band C (Figure 7A), whereas the enhancement in processing by the combination of the two is much less in BHK cells (Supplemental Figure 2). Consistent with the role of the "DAD" motif as the ER exit code in the context of ΔF508 CFTR, the enhanced processing of ΔF508 CFTR by introducing R555K at both 37 and 30°C is abolished by further introduction of DAA mutation (Figure 7B).

To probe the mechanism of R555K rescue of ΔF508 CFTR, we first observed the kinetic accumulation of ΔF508/R555K in bands B and C and compared it with that of ΔF508. Although the rates of accumulation in band B are largely similar between the two forms of CFTR, R555K significantly increases the accumulation of ΔF508 CFTR in band C (Figure 7C), suggesting increased export and/or post-ER stability. CHX chase indicated a moderate increase in the post-ER stability by R555K (Figure 7D), and CFTR quantitative coimmunoprecipitation revealed an increase in association with Sec24 (Figure 7E). These results suggest that R555K rescues ΔF508 CFTR through enhancing both export and post-ER stability.

Rescue of ΔF508 CFTR by Low Temperature or R555K Is Accompanied by the Enhancement in Global Conformational Maturation

We probed domain conformation of ΔF508 CFTR after rescue with low temperature, R555K, or both using in situ limited proteolysis. After incubating HEK293 cells stably expressing ΔF508 CFTR at 30°C for 16 h, we observed a weak but clear appearance of the 37-kDa fragment at the two highest trypsin concentrations when probed with MM13-4 (Figure 8Ab, lanes 7 and 8, black arrowhead), which is characteristic of the mature CFTR (Figures 3Aa and 4A, b and c). However, the pattern of the 42-kDa fragment is largely unchanged (Figure 8A, a and b). This suggests that reducing the temperature promotes the conformational maturation of ΔF508 CFTR. The introduction of R555K has a similar effect (Figure 8Ac), suggesting that R555K substitution alters the folding of ΔF508 CFTR in a way that achieves a comparable level of conformational maturation as the low-temperature rescue.

Although "ΔF508, 30°C", "ΔF508/R555K," and "DAA" have comparable distribution between bands B and C, at the steady state, the relative intensity of the 37-kDa band is higher and the 42-kDa fragments are more resistant to tryp-

Figure 6. ΔF508 CFTR utilizes the "DAD" motif as ER exit code. (A and B) HEK293 cells were transiently transfected with ΔF or ΔF/DAA CFTR and incubated at 37°C. Twenty-four hours after transfection, the cells were incubated at 37°C (A) or 30°C (B) for an additional 16 h before they were lysed. Cell lysates were immunoblotted for CFTR and actin. Multiple exposures were taken to ensure that the intensity of bands C and B lies within the quantifiable range. The properly exposed bands (labeled by arrowheads) were quantified by densitometry. CFTR levels in bands B and C were normalized to actin and then to the values of the ΔF. The means and the SEMs are plotted in the charts. The values for ΔF and ΔF/DAA were compared by two-tailed and unpaired t test. *p ≤ 0.05 and **p ≤ 0.01, n = 3. (C) HEK293 cells were transiently transfected with ΔF or ΔF/DAA CFTR, 20 h after transfection, cells were lysed, and quantitative coimmunoprecipitation was conducted using protein G beads coated with CFTR mAb M3A7. The immunoprecipitated proteins were separated by SDS-PAGE and immunoblotted for Sec24 and CFTR. Mock-transfected HEK293 cells (mock) served as the negative control. The level of the associated Sec24 was first subtracted by that of mock and then normalized to the level of CFTR in band B. Four independent experiments were conducted. To make the data comparable, the Sec24/CFTR-B values for ΔF and ΔF/DAA were expressed as the fraction of each in the sum of the two. **p ≤ 0.01. (D–F) HEK293 cells stably expressing DAA (D), ΔF (E), or ΔF/DAA (F) CFTR were cultured at 37°C for over 24 h followed by incubation at 30°C for the indicated time periods. Cell lysates were immunoblotted for CFTR. For each individual cell line, CFTR levels in bands B and C were quantified, normalized to actin, and then normalized to the value of band B at time 0. (G–H) In situ limited proteolysis was performed on microsomes prepared from HEK293 cells stably expressing ΔF or ΔF/DAA and probed with MM13-4 (G) and M3A7 (H).
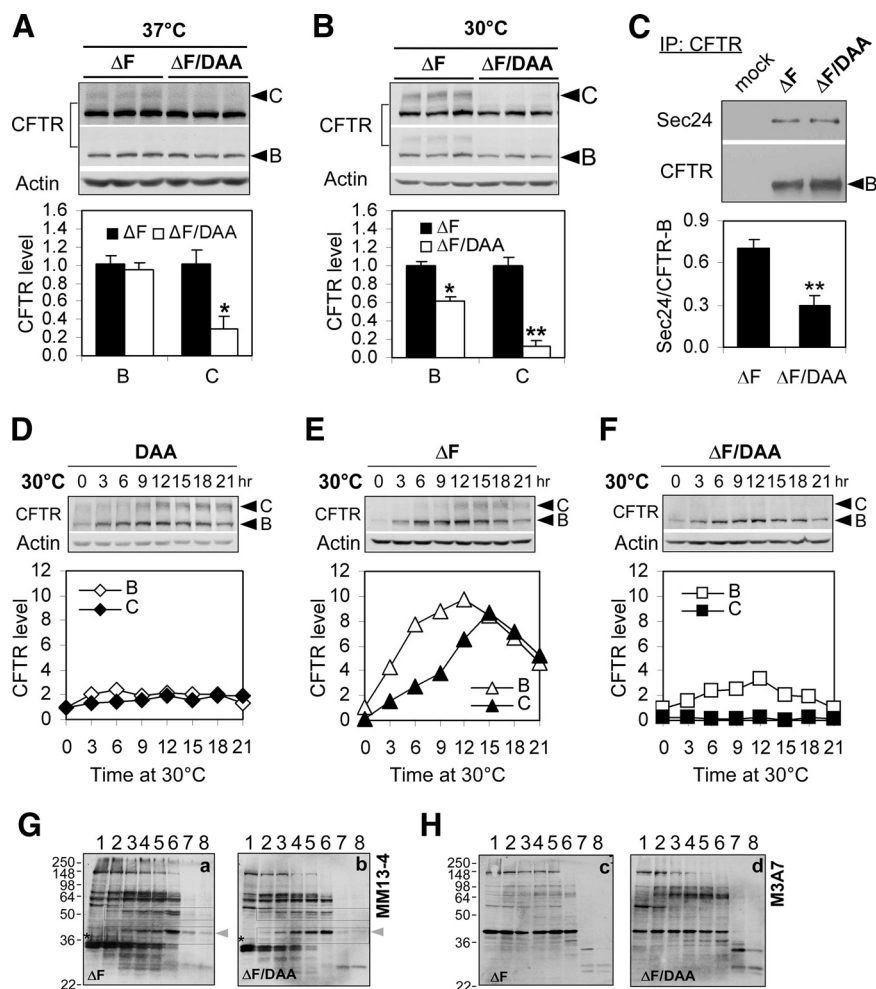
sin in DAA than in the other two (Figures 3Ac and 8A, b and c), suggesting that the degree of conformational maturation of ΔF508 after rescue by either method is still lower than that of DAA, which shares similar conformation with wild-type CFTR.

Notably, when low temperature is combined with R555K in HEK293 cells, we have observed a dramatic increase in the trypsin resistance of the 42-kDa fragments and an increased relative intensity of the 37-kDa band, which together lead to a tryptic pattern similar to wild-type CFTR (Figure 8A, d and e). This is consistent with the additive effects of the two rescue maneuvers on ΔF508 processing in HEK293 cells (Figure 7A).

To assess the impact of ΔF508 rescue on NBD1, we quantified the 50-kDa bands and found that all rescue maneuvers whether individually or in combination restore NBD1 trypsin sensitivity to close to wild-type level (Figure 8B).

When probed with M3A7, we have observed a partial correction of ΔF508 NBD2 conformation by low temperature, as reflected in the coexistence of the 30-kDa band characteristic of wild-type conformation and a number of bands characteristic of ΔF508 conformation (Figure 8A, f, g, and j). This suggests that after low temperature treatment, only a fraction of the ΔF508 molecules achieved conformational maturation. In contrast, R555K substitution results in

a more uniform tryptic pattern (Figure 8Ah). Although the 30-kDa fragment typical of wild-type conformation is now clearly present (black arrowhead), the 34-kDa common band that is present in ΔF508, DAA and wild-type CFTR is greatly diminished (Figure 8A, f–h, gray arrowheads), suggesting that R555K produces an additional conformational change in NBD2. The combination of low temperature and R555K did not produce additional conformational correction in NBD2 over what has been achieved by R555K alone (Figure 8A, h and i).

Taken together, we show that rescue of ΔF508 by low temperature or R555K is associated with improved conformational maturation in multiple domains. The degree of ΔF508 rescue generally correlates with the degree of conformational maturation of the amino terminal module.

At Reduced Temperature, ΔF508 Rescue Is Closely Linked to the Multidomain Conformational Reversion

The efficiency of the temperature rescue of ΔF508 depends on the cellular machinery (Wang *et al.,* 2008). When transiently expressed, HEK293 cells support a slightly higher level of ΔF508 rescue than BHK cells, reflected in a slightly higher C% (from 20 to 42% for HEK293 vs. from 15 to 31% for BHK, Figure 9A, left and middle). However, in BHK-ΔF (Seibert *et al.,* 1995), a specific BHK cell line stably expressing
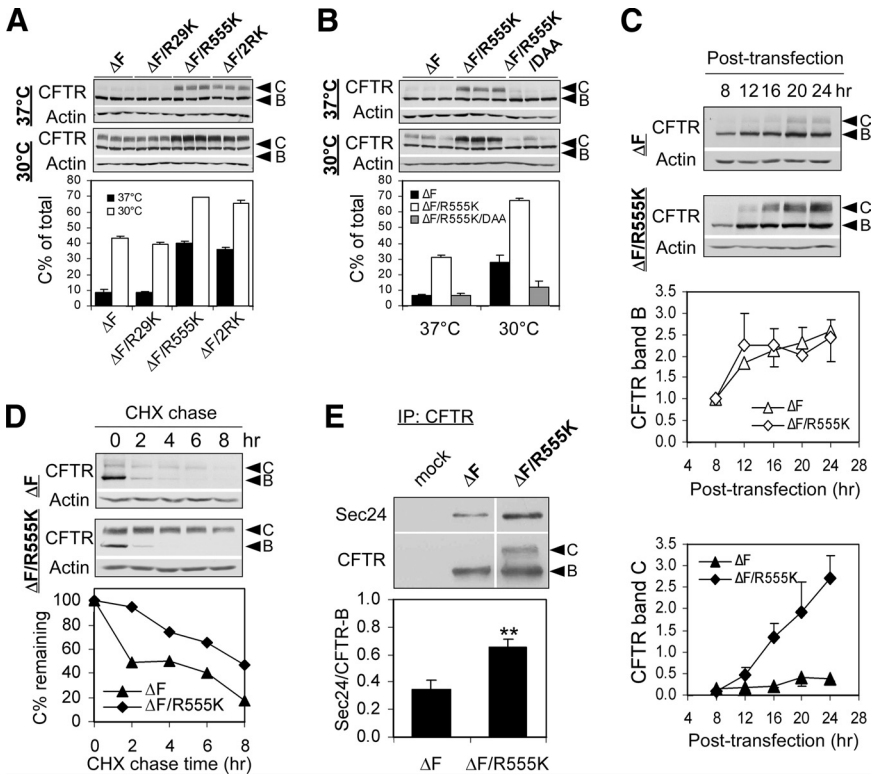
Figure 7. R555K improves export and post-ER stability of ΔF508 CFTR. (A) HEK293 cells were transiently transfected with ΔF, ΔF/R29K, ΔF/R555K and ΔF/R29K/R555K (ΔF/2RK) and cultured at 37°C for 20 h (37°C), or further switched to 30°C and incubated for an additional 16 h (30°). Cell lysates were immunoblotted for CFTR and actin. The level of CFTR in bands B and C was quantified, normalized to actin. The percentage of band C of total (C%) was calculated for each construct, and the means and SEMs were plotted. n = 3. (B) HEK293 cells were transiently transfected with ΔF, ΔF/R555K and ΔF/R555K/DAA CFTR. Transfected cells were incubated at 37°C for 20 h (37°C), or further switched to 30°C and incubated for an additional 16 h at 30°C (30°C) before the cells were lysed. The cell lysates were immunoblotted for CFTR and actin. The quantification of bands and calculation of C% are as described above. n = 3. (C) HEK293 cells were transiently transfected with ΔF or ΔF/R555K CFTR and incubated at 37°C for the indicated time. Cell lysates were immunoblotted for CFTR and actin. Quantification of CFTR in bands B and C was performed as described in Figure 1C. Two independent time courses for each were performed. The representative immunoblotting images are shown on the top, and the means and SEMs are plotted below. (D) CHX chase on HEK293 cells stably expressing ΔF and ΔF/R555K was performed and quantified as described in Figure 2. (E) HEK293 cells were transiently transfected with ΔF or ΔF/R555K. Twenty hours after transfection, the cells were lysed, and quantitative coimmunoprecipitation was conducted as described in Figure 6C. Representative immunoblots are shown on the top, and the means and SEMs of seven experiments are represented in the chart below. **p ≤ 0.01.

ΔF508 CFTR, the temperature rescue is undetectable under the same condition (Figure 9A, right; Wang *et al.*, 2008). To test the relationship between ΔF508 rescue and its domain conformation, we conducted in situ limited proteolysis on microsomes prepared from BHK-WT cells, BHK-ΔF cells incubated at 37 or 30°C, and BHK-ΔF/R555K cells. In BHK cells, similar conformational differences between wild-type and ΔF508 CFTR have been observed. When probed with MM13-4, the 37-kDa fragment was present in wild-type CFTR but not in ΔF508 at high trypsin concentrations, and the 42-kDa fragment is more resistant to trypsin in wild-type CFTR (Figure 9B, a and b). As has been observed in HEK293 cells (Figure 3Ab), a 37-kDa background band was present even in the absence of trypsin (Figure 9B, a–c, lane 1, asterisk), whose density decreases with the increase in trypsin concentration. However, unlike in HEK293 cells (Figure 8A, a and b), the same low-temperature treatment of BHK-ΔF cells failed to increase the density of the 37-kDa fragment at the two highest trypsin concentrations (Figure 9B, b and c, lanes 7 and 8), and this is accompanied by the lack of any increase in ΔF508 processing. In contrast, BHK cells stably expressing ΔF508/R555K showed a clear appearance of the 37-kDa bands at high trypsin concentrations (Figure 9Bd, black arrowhead).

We quantified the 50-kDa bands and found that although low temperature failed to rescue ΔF508 CFTR in BHK-ΔF cells, it caused a moderate shift of the 50-kDa band pattern toward wild-type CFTR (Figure 9C). Obviously such shift alone is not sufficient to produce a global conformational reversion that results in rescue. In contrast, R555K was able to restore the 50-kDa pattern to wild-type level. These data suggest that lowering the temperature does moderately stabilize ΔF508 NBD1 in BHK-ΔF cells but perhaps not sufficient to restore the global conformational defect of ΔF508 CFTR to allow rescue.

When probed with M3A7, the 30-kDa fragment (Figure 9Be, black arrowhead) characteristic of wild-type NBD2 conformation was present in BHK-WT but not in BHK-ΔF (Figure 9Bf). Parallel to the behavior of the amino terminal module, reducing temperature did not lead to the appearance of the 30-kDa fragment (Figure 9Bg) but R555K did (Figure 9Bh).

Taken together, reducing the temperature itself is necessary but not sufficient for the multidomain conformational reversion of ΔF508 CFTR. The actions of the cellular chaperone machinery and/or other biological processes are required to promote the conformational maturation and hence the rescue of ΔF508 CFTR.

DISCUSSION

A great number of mutations in multiple domains of CFTR compromise its processing but the mechanisms are not clear (Cheng *et al.*, 1990; Smit *et al.*, 1995; Seibert *et al.*, 1996, 1997; Vankeerberghen *et al.*, 1998; Ostedgaard *et al.*, 1999; Cormet-Boyaka *et al.*, 2004; Clain *et al.*, 2005; Wang *et al.*, 2007b; Du and Lukacs, 2009). We characterized the residual processing of ΔF508, a conformational mutant, and DAA, an ER exit code mutant. The residual processing of DAA is consistent with the role of the di-acidic code in cargo concentration, the disruption of which dramatically reduces the export kinetics without completely blocking ER exit (Nishimura and Balch, 1997). Pulse-chase analysis is effective in assessing the kinetic processing of CFTR but is not sensitive enough to
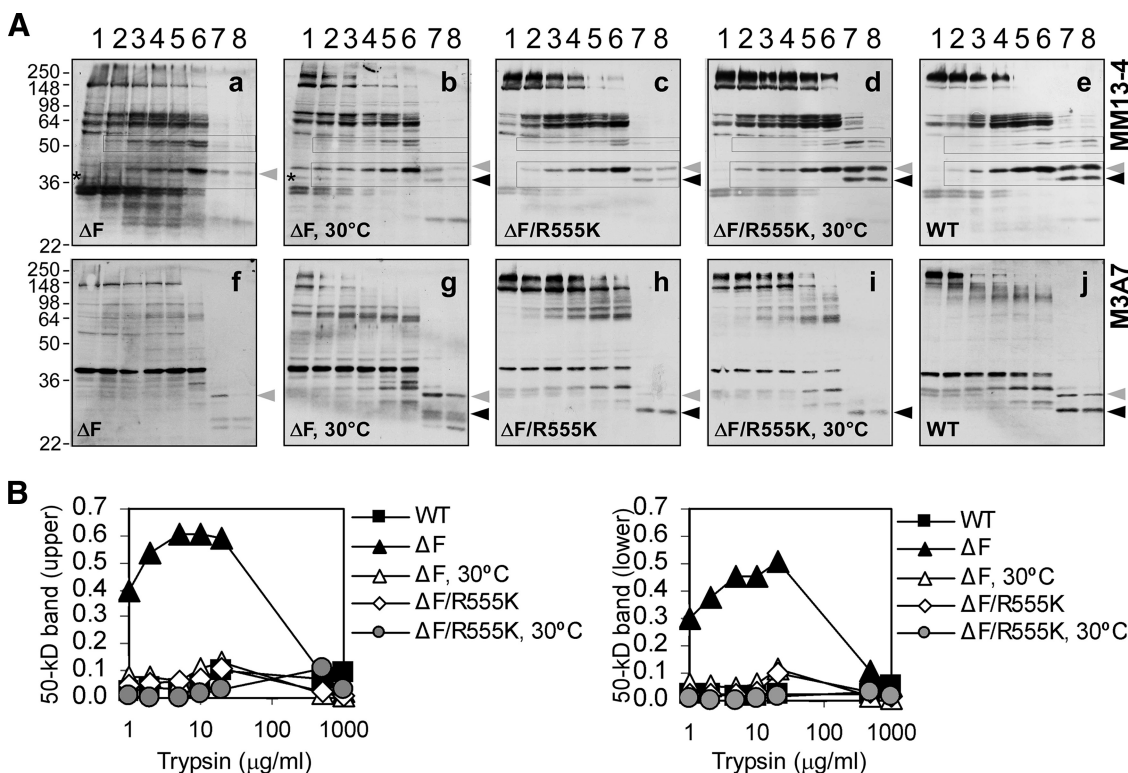
Figure 8. Low temperature and R555K promote the conformational maturation of ΔF508 CFTR in HEK293 cells. (A) Microsomes prepared from HEK293 cells stably expressing the indicated CFTR constructs were subjected to trypsin digestion at increasing concentrations as described in Figure 3. For ΔF, 30°C and ΔF/R555K, 30°C, cells were incubated at 30°C for 16 h before the preparation of microsomes. The digestion mixtures were immunoblotted with CFTR mAb MM13-4 (a–e) or M3A7 (f–j). (B) The ~50-kDa bands in A, a–e, were quantified as described above.

visualize the low-efficiency residual processing of ΔF508 or DAA (Wang *et al.*, 2004). Using a transient expression system, we followed the kinetic accumulation of CFTR in bands B and C over a period of 24–32 h (Figure 1, B and C). This approach dramatically increases the sensitivity and allows quantitative assessment of the extent of processing of CFTR processing mutants. Surprisingly, we found that DAA processes better than ΔF508 CFTR at the steady state (Figure 1A), suggesting that defective ER exit code alone only cause mild CFTR misprocessing at the steady state, whereas conformational defects can cause a far more severe misprocessing phenotype. This is attributable at least in part to the reduction in post-ER stability of ΔF508 CFTR (Figure 2). Previous work has showed that DAA has lower association with Sec24 than ΔF508 (Wang *et al.*, 2004), suggesting a more reduced coupling to COPII. However, whether ΔF508 has additional defects in the ER-to-Golgi transport remains to be determined.

We compared the domain conformation of ΔF508 and DAA using in situ limited proteolysis, and found that although ΔF508 CFTR has global conformational defects, DAA has much limited conformational deviation from wild-type CFTR (Figure 3). A recent study showed that a number of CFTR processing mutations located in different domains display a global conformational change similar to that of ΔF508 (Du and Lukacs, 2009), suggesting the existence of a common link between domain conformation and CFTR processing. These data are consistent with the notion that DAA is a relatively "pure" sorting mutant as opposed to conformation mutants such as ΔF508.

We have noticed a major change in the pattern of the amino terminal 50-kDa tryptic fragments as a result of ΔF508 mutation (Figure 3A, a–c, and B–E). The pattern change is dependent on CFTR conformation rather than the presence of spontaneous degradation intermediates of CFTR. This is supported by the following experimental evidence: 1) Urea wash obscured the pattern difference between wild-type and ΔF508 CFTR (Figure 3, C and E). 2) The pattern differs among DAA CFTR at different stages of maturation (Figure 4). 3) The pattern of ΔF508 CFTR reverts to wild-type-like upon rescue by low temperature or R555K or both in HEK293 cells (Figure 8). 4) The pattern undergoes only partial reversion at low temperature in BHK-ΔF cells that do not support the temperature-dependent rescue of ΔF508 CFTR (Figure 9, B and C).

ΔF508 mutation arrests the conformational maturation of CFTR (Lukacs *et al.*, 1994; Zhang *et al.*, 1998) and therefore has prolonged association with Hsp70 (Yang *et al.*, 1993; Meacham *et al.*, 1999). The partially folded mutant CFTR is believed to be recognized by the ER quality control system, withheld from ER export, and shuttled to the ERAD pathway. In contrast, DAA was found to be able to achieve full global conformational maturation (Figure 4). Consistent with this, its association with Hsp70 is much lower than ΔF508 CFTR (Figure 5).

Because the utilization of sorting signals depends on domain conformation and/or protein–protein interactions, we tested if misfolding within ΔF508 CFTR has altered usage of its ER exit code, and the answer is no (Figure 6). In addition to the "DAD" ER exit code (Wang *et al.*, 2004), RXR ER
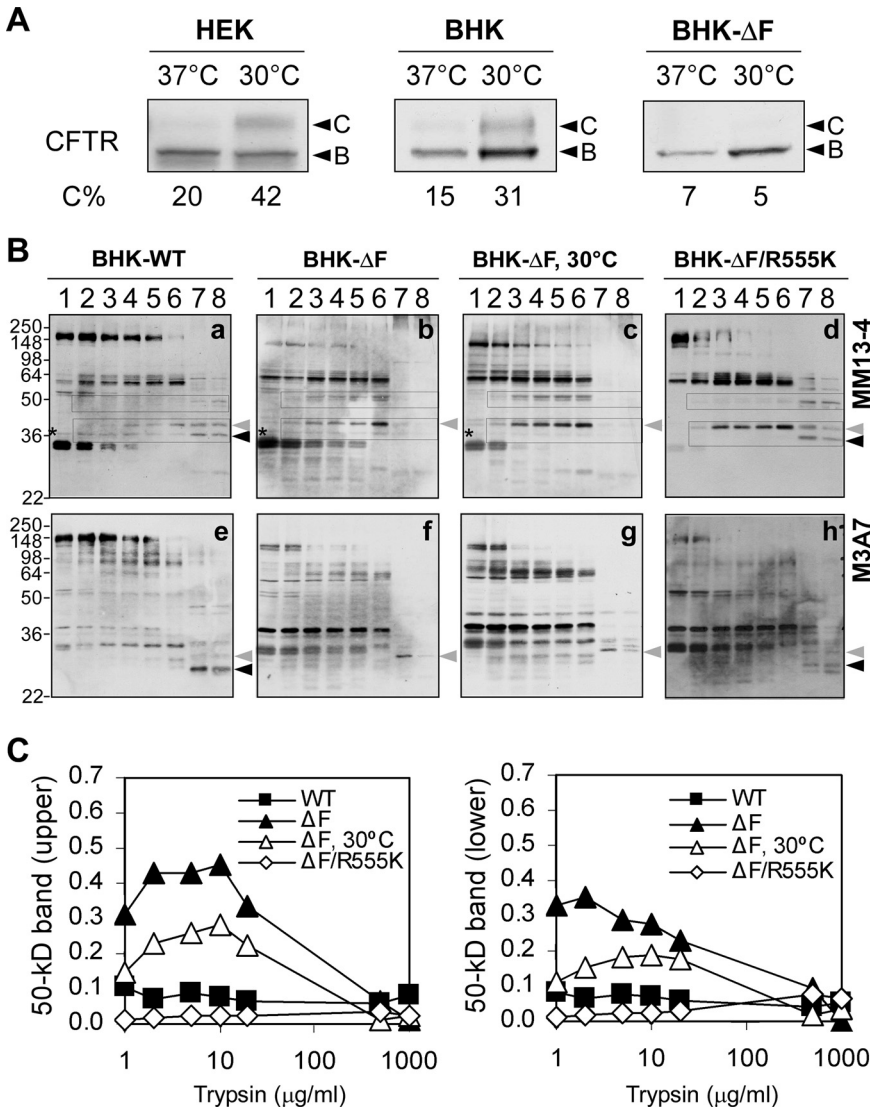
Figure 9. The cell line-dependent temperature rescue of ΔF508 correlates with global conformational reversion in CFTR. (A) HEK293 (HEK) and BHK cells were transiently transfected with ΔF508 CFTR. After incubation at 37°C for over 24 h, the cells were either maintained at 37°C, or shifted to 30°C and incubated for another 16 h (30°C). The BHK-ΔF cells were cultured at 37°C for over 24 h before it was either maintained at the same temperature (37°C) or shifted to 30°C and incubated for another 16 h (30°C). The cells were lysed, and lysates were immunoblotted for CFTR. CFTR level in bands B and C were quantified, and C% was calculated as described above. (B) In situ limited proteolysis was conducted on microsomes prepared from the indicated BHK stable cell lines as described in Figures 3. For BHK-ΔF, 30°C, BHK-ΔF cells were incubated at 30°C for 16 h before microsome preparation. The trypsin digestion mixtures were probed with CFTR mAb MM13-4 (a–d) or M3A7 (e–h). (C) The ~50-kDa bands in B, a–d, were quantified as described above.

retention/retrieval motifs have been identified in CFTR (Chang *et al.*, 1999; Hegedus *et al.*, 2006). The ER accumulation of ΔF508 can be caused by failure to exit or by active retention/retrieval. ΔF508 CFTR has reduced coupling to Sec24, which is reversed by low temperature (Wang *et al.*, 2004, 2008) or R555K (Figure 7E). These together suggest a defect at or before the coupling of CFTR to COPII. Consistent with this, a mutation in yeast ABC transporter Yor1p that is homologous to ΔF508 in CFTR prevents Yor1p from being packaged into COPII vesicles in vitro (Pagant *et al.*, 2007).

Do the RXR motifs play a significant role in the ER accumulation of ΔF508 CFTR? We found that R29K does not contribute to ΔF508 rescue in HEK 293 cells (Figure 7A) but slightly improves ΔF508 rescue only in combination with R555K in BHK cells (Supplemental Figure 2). R555K rescues ΔF508 CFTR by improving its coupling to COPII and moderately increasing its post-ER stability (Figure 7, D and E). These are accompanied by improved global conformational maturation (Figure 8). Interestingly, R553M, the substitution of the other arginine in the same RXR motif, rescues ΔF508 CFTR as well (Teem *et al.*, 1993), but through enhancing the folding yield of ΔF508 NBD1 based on an in vitro study (Qu

et al., 1997). In fact, ΔF508 can be rescued by a number of other substitutions within NBD1 (Teem *et al.*, 1993, 1996; DeCarvalho *et al.*, 2002; Roxo-Rosa *et al.*, 2006; Wang *et al.*, 2007b; Pissarra *et al.*, 2008), the mechanisms of which remain to be understood. Although substitution of either arginine in the RXR motif at residues 553–555 rescues ΔF508 CFTR, our data do not support the utilization of this RXR motif as a dominant ER retention signal in the context of ΔF508 misprocessing and rescue. Instead, like other second site mutations in NBD1, R555K and R553M substitutions might alter the conformation of CFTR in a way that repairs ΔF508 conformation defects.

The ER exit code "DAD", F508, and many ΔF508 rescuing mutations (including R555K and R553M) reside in NBD1. Paradoxically, no major conformational change has been detected in ΔF508 NBD1 by structural analysis (Lewis *et al.*, 2005; Thibodeau *et al.*, 2005). This is partly attributable to the inclusion of multiple "solubilization mutations" into ΔF508 NBD1 to facilitate its purification (Lewis *et al.*, 2005), several of which, including R555K, rescue the ΔF508 export and channel gating defects (Pissarra *et al.*, 2008). Based on biophysical analysis of the chemical folding of the isolated NBD1 (Qu and Thomas, 1996; Qu *et al.*, 1997), the recent

computational simulation of NBD1 (Serohijos *et al.,* 2008b), and in situ limited proteolysis (Figures 3, 8, and 9), it is clear that the deletion of F508 does cause defective folding in this critical domain. We observed a clear correlation between NBD1 conformation and the state of CFTR maturation (Figure 4), between NBD1 conformation and CFTR global conformation (Figure 9), and further between CFTR global conformation and ΔF508 rescue (Figures 8 and 9). These together suggest a critical role for NBD1 in cooperative domain assembly and processing of CFTR (Du and Lukacs, 2009). Although ΔF508 mutation initiates a global conformational change from NBD1, R555K, originating in same domain, reverses the global conformational defect. The same phenomenon has been observed in both HEK293 and BHK cells (Figures 8 and 9).

Reducing the temperature produces a similar effect on ΔF508 CFTR conformation as R555K in HEK293 cells (Figure 8). HEK293 cells and BHK cells display slightly different efficiency of ΔF508 rescue at reduced temperature (Figure 9A, left and middle). This reflects certain differences between the two cell lines in various aspects of CFTR biogenesis. However, BHK-ΔF, a specific BHK cell line stably expressing ΔF508 CFTR, fails to display any detectable rescue of ΔF508 CFTR at low temperature (Figure 9A, right). Although the mechanism underlying this loss of rescue in BHK-ΔF is not entirely clear, altered association of cytoplasmic chaperones with ΔF508 CFTR after the temperature downshift has been observed, suggesting differences in the functionality of the chaperone machinery (Wang *et al.,* 2008). We used this BHK-ΔF cell line as a tool to probe the relationship between CFTR domain conformation and ΔF508 rescue. In BHK-ΔF cells, we observed only a partial conformational reversion in NBD1, which is apparently insufficient to trigger the global conformational reversion necessary for ΔF508 rescue (Figure 9). We have not conducted in situ limited proteolysis on microsomes derived from BHK cells transiently transfected with ΔF508 CFTR after incubation at reduced temperature. As under such conditions ΔF508 CFTR rescue does occur albeit at slightly lower efficiency (Figure 9A, middle), we expect that global conformational reversion also occurs but to a lesser extent than in HEK293 cells.

From our analyses, it is clear that there is an intricate interplay between the ER exit code and domain conformation in CFTR misprocessing and rescue. DAA is a rare example where domain conformation has very limited contribution to its misprocessing. Even in this case, we have observed a global maturation-dependent conformational conversion (Figure 4). ΔF508, on the other hand, have severe global conformational defect, which reduces its coupling to COPII (Wang *et al.,* 2004), reduces its post-ER stability and impairs its channel gating. These lead to a severe deficiency in CFTR function at the plasma membrane. Rescue maneuvers such as low temperature and R555K restore both its ER export (Figure 7E; Wang *et al.,* 2004) and post-ER stability (Figure 7D; Sharma *et al.,* 2001; Varga *et al.,* 2008), and these processes are highly dependent upon the ER exit code "DAD" (Figures 6 and 7B).

The conformation-dependent processing of CFTR has significant implications in CF drug discovery. ΔF508 CFTR has defects in ER export (Cheng *et al.,* 1990), cell surface stability (Lukacs *et al.,* 1993), and channel gating (Dalemans *et al.,* 1991), because of its wide-spread conformational defects (Zhang *et al.,* 1998; Chen *et al.,* 2004; Du *et al.,* 2005; Cui *et al.,* 2007; Rosser *et al.,* 2008; Serohijos *et al.,* 2008a; Du and Lukacs, 2009). Correcting its global conformational defects may simultaneously improve export, stability, and channel

gating, leading to a dramatic increase in chloride conductance across the plasma membrane. R555K improves the ER export (Figure 7E), post-ER stability (Figure 7D), and channel gating (Teem *et al.,* 1996) of ΔF508 CFTR. Certain small molecule correctors improve cell surface localization of ΔF508 CFTR by increasing both ER export and cell surface stability (Pedemonte *et al.,* 2005; Varga *et al.,* 2008), whereas others can improve both processing and channel activity (Wang *et al.,* 2006b).

The cell surface localization and functioning of ΔF508 CFTR can be greatly enhanced by improving the folding of NBD1 and its interactions with other domains. Small molecule correctors can be generated through rational molecular design or high throughput screening (Pedemonte *et al.,* 2005; Van Goor *et al.,* 2006; Carlile *et al.,* 2007) that bind directly to CFTR and alter its conformation (Wang *et al.,* 2007b). The chaperone machinery can be modified in a way that further favors the cellular rescue of ΔF508 CFTR (Wright *et al.,* 2004; Wang *et al.,* 2006a). Combining R555K with low-temperature additively improves the conformational maturation of ΔF508 CFTR (Figure 8) and its processing (Figure 7A) in HEK293 cells. Such effect is dependent upon cellular chaperone machinery as the additive effect is much reduced in BHK cells (Supplemental Figure 2). Therefore, combinational approaches (Wang *et al.,* 2007a) aimed at the global conformational correction of ΔF508 CFTR have a great potential in the development of therapeutics for CF patients.

REFERENCES

Aridor, M., Weissman, J., Bannykh, S., Nuoffer, C., and Balch, W. E. (1998). Cargo selection by the COPII budding machinery during export from the ER. J. Cell Biol. *141*, 61–70.

Barlowe, C., Orci, L., Yeung, T., Hosobuchi, M., Hamamoto, S., Salama, N., Rexach, M. F., Ravazzola, M., Amherdt, M., and Schekman, R. (1994). COPII: a membrane coat formed by Sec proteins that drive vesicle budding from the endoplasmic reticulum. Cell *77*, 895–907.

Carlile, G. W., Robert, R., Zhang, D., Teske, K. A., Luo, Y., Hanrahan, J. W., and Thomas, D. Y. (2007). Correctors of protein trafficking defects identified by a novel high-throughput screening assay. Chembiochemistry *8*, 1012–1020.

Chang, X. B., Cui, L., Hou, Y. X., Jensen, T. J., Aleksandrov, A. A., Mengos, A., and Riordan, J. R. (1999). Removal of multiple arginine-framed trafficking signals overcomes misprocessing of delta F508 CFTR present in most patients with cystic fibrosis. Mol. Cell *4*, 137–142.

Chen, E. Y., Bartlett, M. C., Loo, T. W., and Clarke, D. M. (2004). The DeltaF508 mutation disrupts packing of the transmembrane segments of the cystic fibrosis transmembrane conductance regulator. J. Biol. Chem. *279*, 39620–39627.

Cheng, S. H., Gregory, R. J., Marshall, J., Paul, S., Souza, D. W., White, G. A., O'Riordan, C. R., and Smith, A. E. (1990). Defective intracellular transport and processing of CFTR is the molecular basis of most cystic fibrosis. Cell *63*, 827–834.

Clain, J., *et al.* (2005). Misprocessing of the CFTR protein leads to mild cystic fibrosis phenotype. Hum. Mutat. *25*, 360–371.

Cormet-Boyaka, E., Jablonsky, M., Naren, A. P., Jackson, P. L., Muccio, D. D., and Kirk, K. L. (2004). Rescuing cystic fibrosis transmembrane conductance regulator (CFTR)-processing mutants by transcomplementation. Proc. Natl. Acad. Sci. USA *101*, 8221–8226.

Cui, L., *et al.* (2007). Domain interdependence in the biosynthetic assembly of CFTR. J. Mol. Biol. *365*, 981–994.

Dalemans, W., Barbry, P., Champigny, G., Jallat, S., Dott, K., Dreyer, D., Crystal, R. G., Pavirani, A., Lecocq, J. P., and Lazdunski, M. (1991). Altered chloride ion channel kinetics associated with the delta F508 cystic fibrosis mutation. Nature *354*, 526–528.

DeCarvalho, A. C., Gansheroff, L. J., and Teem, J. L. (2002). Mutations in the nucleotide binding domain 1 signature motif region rescue processing and functional defects of cystic fibrosis transmembrane conductance regulator delta f508. J. Biol. Chem. *277*, 35896–35905.

Denning, G. M., Anderson, M. P., Amara, J. F., Marshall, J., Smith, A. E., and Welsh, M. J. (1992). Processing of mutant cystic fibrosis transmembrane conductance regulator is temperature-sensitive. Nature *358*, 761–764.

Du, K., and Lukacs, G. L. (2009). Cooperative assembly and misfolding of CFTR domains in vivo. Mol. Biol. Cell *20*, 1903–1915.

Du, K., Sharma, M., and Lukacs, G. L. (2005). The DeltaF508 cystic fibrosis mutation impairs domain-domain interactions and arrests post-translational folding of CFTR. Nat. Struct. Mol. Biol. *12*, 17–25.

Hegedus, T., Aleksandrov, A., Cui, L., Gentzsch, M., Chang, X. B., and Riordan, J. R. (2006). F508del CFTR with two altered RXR motifs escapes from ER quality control but its channel activity is thermally sensitive. Biochim. Biophys. Acta *1758*, 565–572.

Jensen, T. J., Loo, M. A., Pind, S., Williams, D. B., Goldberg, A. L., and Riordan, J. R. (1995). Multiple proteolytic systems, including the proteasome, contribute to CFTR processing. Cell *83*, 129–135.

Kleizen, B., van Vlijmen, T., de Jonge, H. R., and Braakman, I. (2005). Folding of CFTR is predominantly cotranslational. Mol. Cell *20*, 277–287.

Lewis, H. A., *et al.* (2005). Impact of the deltaF508 mutation in first nucleotide-binding domain of human cystic fibrosis transmembrane conductance regulator on domain folding and structure. J. Biol. Chem. *280*, 1346–1353.

Lukacs, G. L., Chang, X. B., Bear, C., Kartner, N., Mohamed, A., Riordan, J. R., and Grinstein, S. (1993). The delta F508 mutation decreases the stability of cystic fibrosis transmembrane conductance regulator in the plasma membrane. Determination of functional half-lives on transfected cells. J. Biol. Chem. *268*, 21592–21598.

Lukacs, G. L., Mohamed, A., Kartner, N., Chang, X. B., Riordan, J. R., and Grinstein, S. (1994). Conformational maturation of CFTR but not its mutant counterpart (delta F508) occurs in the endoplasmic reticulum and requires ATP. EMBO J. *13*, 6076–6086.

Meacham, G. C., Lu, Z., King, S., Sorscher, E., Tousson, A., and Cyr, D. M. (1999). The Hdj-2/Hsc70 chaperone pair facilitates early steps in CFTR biogenesis. EMBO J. *18*, 1492–1505.

Miller, E., Antonny, B., Hamamoto, S., and Schekman, R. (2002). Cargo selection into COPII vesicles is driven by the Sec24p subunit. EMBO J. *21*, 6105–6113.

Mossessova, E., Bickford, L. C., and Goldberg, J. (2003). SNARE selectivity of the COPII coat. Cell *114*, 483–495.

Nishimura, N., and Balch, W. E. (1997). A di-acidic signal required for selective export from the endoplasmic reticulum. Science *277*, 556–558.

Ostedgaard, L. S., Zeiher, B., and Welsh, M. J. (1999). Processing of CFTR bearing the P574H mutation differs from wild-type and deltaF508-CFTR. J. Cell Sci. *112*(Pt 13), 2091–2098.

Pagant, S., Kung, L., Dorrington, M., Lee, M. C., and Miller, E. A. (2007). Inhibiting endoplasmic reticulum (ER)-associated degradation of misfolded Yor1p does not permit ER export despite the presence of a diacidic sorting signal. Mol. Biol. Cell *18*, 3398–3413.

Pedemonte, N., Lukacs, G. L., Du, K., Caci, E., Zegarra-Moran, O., Galietta, L. J., and Verkman, A. S. (2005). Small-molecule correctors of defective DeltaF508-CFTR cellular processing identified by high-throughput screening. J. Clin. Invest. *115*, 2564–2571.

Pissarra, L. S., Farinha, C. M., Xu, Z., Schmidt, A., Thibodeau, P. H., Cai, Z., Thomas, P. J., Sheppard, D. N., and Amaral, M. D. (2008). Solubilizing mutations used to crystallize one CFTR domain attenuate the trafficking and channel defects caused by the major cystic fibrosis mutation. Chem. Biol. *15*, 62–69.

Plutner, H., Gurkan, C., Wang, X., Lapointe, P., and Balch, W. E. (2005). Microsome-based assay of endoplasmic reticulum to Golgi transport in mammalian cells. In: Cell Biology: A Laboratory Handbook, Vol. 2, ed. J. Celis, San Diego: Elsevier, 209–214.

Qu, B. H., Strickland, E. H., and Thomas, P. J. (1997). Localization and suppression of a kinetic defect in cystic fibrosis transmembrane conductance regulator folding. J. Biol. Chem. *272*, 15739–15744.

Qu, B. H., and Thomas, P. J. (1996). Alteration of the cystic fibrosis transmembrane conductance regulator folding pathway. J. Biol. Chem. *271*, 7261–7264.

Riordan, J. R., *et al.* (1989). Identification of the cystic fibrosis gene: cloning and characterization of complementary DNA. Science *245*, 1066–1073.

Rosser, M. F., Grove, D. E., Chen, L., and Cyr, D. M. (2008). Assembly and misassembly of cystic fibrosis transmembrane conductance regulator: folding

defects caused by deletion of F508 occur before and after the calnexin-dependent association of membrane spanning domain (MSD) 1 and MSD2. Mol. Biol. Cell *19*, 4570–4579.

Roxo-Rosa, M., Xu, Z., Schmidt, A., Neto, M., Cai, Z., Soares, C. M., Sheppard, D. N., and Amaral, M. D. (2006). Revertant mutants G550E and 4RK rescue cystic fibrosis mutants in the first nucleotide-binding domain of CFTR by different mechanisms. Proc. Natl. Acad. Sci. USA *103*, 17891–17896.

Seibert, F. S., Jia, Y., Mathews, C. J., Hanrahan, J. W., Riordan, J. R., Loo, T. W., and Clarke, D. M. (1997). Disease-associated mutations in cytoplasmic loops 1 and 2 of cystic fibrosis transmembrane conductance regulator impede processing or opening of the channel. Biochemistry *36*, 11966–11974.

Seibert, F. S., Linsdell, P., Loo, T. W., Hanrahan, J. W., Clarke, D. M., and Riordan, J. R. (1996). Disease-associated mutations in the fourth cytoplasmic loop of cystic fibrosis transmembrane conductance regulator compromise biosynthetic processing and chloride channel activity. J. Biol. Chem. *271*, 15139–15145.

Seibert, F. S., Tabcharani, J. A., Chang, X. B., Dulhanty, A. M., Mathews, C., Hanrahan, J. W., and Riordan, J. R. (1995). cAMP-dependent protein kinase-mediated phosphorylation of cystic fibrosis transmembrane conductance regulator residue Ser-753 and its role in channel activation. J. Biol. Chem. *270*, 2158–2162.

Serohijos, A. W., Hegedus, T., Aleksandrov, A. A., He, L., Cui, L., Dokholyan, N. V., and Riordan, J. R. (2008a). Phenylalanine-508 mediates a cytoplasmic-membrane domain contact in the CFTR 3D structure crucial to assembly and channel function. Proc. Natl. Acad. Sci. USA *105*, 3256–3261.

Serohijos, A. W., Hegedus, T., Riordan, J. R., and Dokholyan, N. V. (2008b). Diminished self-chaperoning activity of the DeltaF508 mutant of CFTR results in protein misfolding. PLoS Comput. Biol. *4*, e1000008.

Sharma, M., Benharouga, M., Hu, W., and Lukacs, G. L. (2001). Conformational and temperature-sensitive stability defects of the delta F508 cystic fibrosis transmembrane conductance regulator in post-endoplasmic reticulum compartments. J. Biol. Chem. *276*, 8942–8950.

Silvis, M. R., Picciano, J. A., Bertrand, C., Weixel, K., Bridges, R. J., and Bradbury, N. A. (2003). A mutation in the cystic fibrosis transmembrane conductance regulator generates a novel internalization sequence and enhances endocytic rates. J. Biol. Chem. *278*, 11554–11560.

Smit, L. S., *et al.* (1995). Missense mutation (G480C) in the CFTR gene associated with protein mislocalization but normal chloride channel activity. Hum. Mol. Genet. *4*, 269–273.

Teem, J. L., Berger, H. A., Ostedgaard, L. S., Rich, D. P., Tsui, L. C., and Welsh, M. J. (1993). Identification of revertants for the cystic fibrosis delta F508 mutation using STE6-CFTR chimeras in yeast. Cell *73*, 335–346.

Teem, J. L., Carson, M. R., and Welsh, M. J. (1996). Mutation of R555 in CFTR-delta F508 enhances function and partially corrects defective processing. Receptors Channels *4*, 63–72.

Thibodeau, P. H., Brautigam, C. A., Machius, M., and Thomas, P. J. (2005). Side chain and backbone contributions of Phe508 to CFTR folding. Nat. Struct. Mol. Biol. *12*, 10–16.

Van Goor, F., *et al.* (2006). Rescue of {Delta}F508-CFTR trafficking and gating in human cystic fibrosis airway primary cultures by small molecules. Am. J. Physiol. Lung Cell Mol. Physiol. *290*, L1117–L1130.

Vankeerberghen, A., Wei, L., Jaspers, M., Cassiman, J. J., Nilius, B., and Cuppens, H. (1998). Characterization of 19 disease-associated missense mutations in the regulatory domain of the cystic fibrosis transmembrane conductance regulator. Hum. Mol. Genet. *7*, 1761–1769.

Varga, K., Goldstein, R. F., Jurkuvenaite, A., Chen, L., Matalon, S., Sorscher, E. J., Bebok, Z., and Collawn, J. F. (2008). Enhanced cell-surface stability of rescued DeltaF508 cystic fibrosis transmembrane conductance regulator (CFTR) by pharmacological chaperones. Biochem. J. *410*, 555–564.

Wang, X., Koulov, A. V., Kellner, W. A., Riordan, J. R., and Balch, W. E. (2008). Chemical and biological folding contribute to temperature-sensitive DeltaF508 CFTR trafficking. Traffic *9*, 1878–1893.

Wang, X., Matteson, J., An, Y., Moyer, B., Yoo, J. S., Bannykh, S., Wilson, I. A., Riordan, J. R., and Balch, W. E. (2004). COPII-dependent export of cystic fibrosis transmembrane conductance regulator from the ER uses a di-acidic exit code. J. Cell Biol. *167*, 65–74.

Wang, X., *et al.* (2006a). Hsp90 cochaperone Aha1 downregulation rescues misfolding of CFTR in cystic fibrosis. Cell *127*, 803–815.

Wang, Y., Bartlett, M. C., Loo, T. W., and Clarke, D. M. (2006b). Specific rescue of cystic fibrosis transmembrane conductance regulator processing mutants using pharmacological chaperones. Mol. Pharmacol. *70*, 297–302.

Wang, Y., Loo, T. W., Bartlett, M. C., and Clarke, D. M. (2007a). Additive effect of multiple pharmacological chaperones on maturation of CFTR processing mutants. Biochem. J. *406*, 257–263.

Wang, Y., Loo, T. W., Bartlett, M. C., and Clarke, D. M. (2007b). Correctors promote maturation of cystic fibrosis transmembrane conductance regulator (CFTR)-processing mutants by binding to the protein. J. Biol. Chem. *282*, 33247–33251.

Ward, C. L., Omura, S., and Kopito, R. R. (1995). Degradation of CFTR by the ubiquitin-proteasome pathway. Cell *83*, 121–127.

Wright, J. M., Zeitlin, P. L., Cebotaru, L., Guggino, S. E., and Guggino, W. B. (2004). Gene expression profile analysis of 4-phenylbutyrate treatment of IB3–1 bronchial epithelial cell line demonstrates a major influence on heat-shock proteins. Physiol. Genom. *16*, 204–211.

Yang, Y., Janich, S., Cohn, J. A., and Wilson, J. M. (1993). The common variant of cystic fibrosis transmembrane conductance regulator is recognized by hsp70 and degraded in a pre-Golgi nonlysosomal compartment. Proc. Natl. Acad. Sci. USA *90*, 9480–9484.

Zerangue, N., Schwappach, B., Jan, Y. N., and Jan, L. Y. (1999). A new ER trafficking signal regulates the subunit stoichiometry of plasma membrane K(ATP) channels. Neuron *22*, 537–548.

Zhang, F., Kartner, N., and Lukacs, G. L. (1998). Limited proteolysis as a probe for arrested conformational maturation of delta F508 CFTR. Nat. Struct. Biol. *5*, 180–183.